Pa04-051

Oriented Event Shapes in Hadronic Z Decays

The ALEPH Collaboration

Abstract

Using about 4 million events recorded with the ALEPH detector at LEP I, distributions of various event-shape variables are measured as a function of the polar angle of the thrust axis with respect to the e^+e^- beam direction $\cos\theta$. New calculations which include the event orientation are fitted to the data yielding a measurement of the strong coupling constant α_s. The result is compared to that obtained from unoriented event-shape distributions. Preliminary results on α_s and on the size of the QCD corrections to the angular distribution are given.

(Contribution to the International Conference on high Energy Physics Warsaw, Poland, 25-31 July 1996)

1 Introduction

The analysis of event shapes in the process $e^+ e^- \to hadrons$ has corroborated the theory of strong interactions, QCD, and has provided accurate measurements of its strong coupling constant α_s. Usually both experimental distributions and theoretical calculations are integrated over the scattering angle θ, the angle between the beam and the thrust axis. In this paper the event orientation is retained and the distributions of the event-shape variables Y_3, thrust, wide jet broadening and heavy jet mass are measured as function of $\cos\theta$ and compared to next-to-leading order QCD predictions. Using this calculation the strong coupling constant is determined and compared to a measurement based on event shapes integrated over the orientation. Note that the measurements of α_s presented here suffer from the missing resummed prediction in the two-jet region. Therefore it is used only for a check of the oriented calculations. Finally, after integration over the event shapes, the QCD effects on the event orientation itself are analyzed. Similar studies have been performed both at the Z resonance [1], [2] and at lower energies [3]. Higher order QCD corrections are predicted to flatten the distribution of $\cos\theta$ for $Z \to q\overline{q}$, which is proportional to $1 + \cos^2\theta$.

2 Detector and Data Sample

The ALEPH detector is described in detail in [4] and its performance in [5]. Hadronic events are selected requiring at least 6 well measured tracks whose total energy exceeds 15 GeV. A track is defined as well measured when the angle to the beam axis is greater then 18.2°, there are at least four TPC points used for the fit of the track, and it passes through a cylinder centered around the fitted interaction point with a radius of 2 cm and a length of 10 cm. The total visible energy of neutral and charged particles must exceed 45 GeV, and the thrust-axis is required to be well contained within the detector acceptance, i.e. $\cos\theta \leq 0.9$. The thrust-axis does not distinguish between the forward and backward directions, so it is chosen with $\cos\theta \geq 0$, and $\cos\theta$ is called the event orientation. The selection efficiency is 87%, and the background is about 0.2 % stemming from $Z \to \tau^+\tau^-$ and two-photon events. After these cuts, about 3.6×10^6 hadronic events recorded in 1991 to 1995 remain for further analysis.

3 Analysis of Oriented Event Shapes

3.1 Definition of Variables and Theoretical Predictions

The event shape variable Y_3 is defined using the Durham [6] jet-finding algorithm, in which the distance between particles or clusters is given by $y_{ij} = 2\min(E_i^2, E_j^2)(1 - \cos\theta_{ij})/E_{\rm vis}^2$, where $E_{\rm vis}^2$ denotes the visible energy and i, j are the indices of charged tracks and neutral objects reconstructed by the ALEPH tracking system and the calorimeters. All particles are clustered until 3 jets remain, and Y_3 is the smallest y_{ij} built with these jets. Thrust is defined by $T_R = \max\left(\sum_i \mid \vec{P}_i.\vec{n}_T \mid / \sum_i \mid \vec{P}_i \mid\right)$ where $\vec{n}_T$ is the thrust-axis. For the wide jet broadening B_W each event is divided into two hemispheres $S_\pm$ according to the thrust axis. The quantities $B_\pm = \sum_{i \in S_\pm} \mid \vec{P}_i \times \vec{n}_T \mid /2\sum_i \mid \vec{P}_i \mid$ are calculated and $B_W = \max(B_+, B_-)$. The same definition of hemispheres applies for the heavy jet mass M_H. The invariant mass in each hemispheres is calculated and the larger one is called M_H.

All numerical calculations are done at the level of partons using a Monte Carlo program `EVENT2` [7] based on the dipole formalism [8] for the integration of the $\mathcal{O}(\alpha_s^2)$ matrix elements. In this framework the double differential cross section can be written as follows:

$$\frac{1}{\sigma}\frac{d^2\sigma(X,\cos\theta)}{dX\,d\cos\theta} = \frac{\alpha_s(\mu^2)}{2\pi}A(X,\cos\theta) + \left(\frac{\alpha_s(\mu^2)}{2\pi}\right)^2\left[A(X,\cos\theta)2\pi b_0\ln\left(\frac{\mu^2}{s}\right)+B(X,\cos\theta)\right] \quad , \qquad (1)$$

where

$$b_0 = \frac{33-2n_f}{12\pi}\ ,\ X = Y_3, T_R, B_W, M_H \quad .$$

Here, μ is the renormalization scale, and the coefficients A and B have been computed [7].

3.2 Correction Procedure

Since the theoretical prediction is valid only at the level of partons, corrections are needed for the effects of initial state radiation, hadronization, geometrical acceptance, detector efficiency and resolution. Corrections are applied to the theoretical distributions by means of bin-by-bin multiplicative factors. The correction factors are obtained from various Monte Carlo models. Hadronization corrections have been computed with the generators JETSET [9] using both the parton shower (PS) and the $\mathcal{O}(\alpha_s^2)$ matrix element option (ME), with HERWIG (HW) [10] and with ARIADNE (AR) [11]. The important parameters of these models have been tuned to reproduce globally measured quantities. Acceptance and resolution corrections are estimated with a Monte Carlo detector simulation. Finally, theory and experiment are compared at the level of the detector, all corrections being applied to the theoretical expectation.

3.3 Simultaneous Analysis of Event Shapes and Orientation

Oriented event-shape distributions are measured in nine bins of $\cos\theta$ between 0.1 and 0.9. The theoretical prediction of the formula (1) is fitted to the data by means of a least squares minimization with $\alpha_s(M_Z^2)$ as free parameter. The renormalization scale μ is set to $M_Z/2$. In order to obtain a good description of the data, the two-jet region has to be excluded from the fit, which is based on second order calculations only. The fit range has been put in the central region of the distribution where the correction factors are close to unity.
In a first step, α_s is determined in each bin of $\cos\theta$. The result is shown in Fig. 1. No systematic dependence on $\cos\theta$ is found.
Subsequently the fit is repeated for all bins of $\cos\theta$ simultaneously. The total χ^2 of the simultaneous fit increases less than 10 % with respect to the χ^2 of the fit with individual values of α_s in each bin of $\cos\theta$. The two-dimensional distribution can be described by a unique value of α_s and the results for each variable are given in Table 1. As an example the thrust distribution is shown in Fig. 2, together with the result of the fit, for different bins of $\cos\theta$.
In order to check the reliability of the method, the event-shape distributions have been integrated over $\cos\theta$, and α_s has been determined using the integrated $\mathcal{O}(\alpha_s^2)$ prediction. An example of the fit is shown in Fig. 3 and the results are given in Table 3. The central values of α_s are in good agreement with those obtained from oriented event shapes, and the systematic uncertainties, to be described in the following section, are also similar.

3.4 Systematic Studies

The uncertainty on the hadronization model used to compute corrections has been estimated by the four models above. The results given in Table 1 are the mean values of α_s. Half of the maximum discrepancy between any of the models is given as systematic uncertainty.
The main uncertainty related to fixed order perturbation theory is due to the choice of the renormalization scale. The latter one is put by default to $M_Z/2$ and has been varied from the mass of the b-quark to the mass of the Z-boson.

Possible impacts of Bose-Einstein correlations on event shapes are conservatively derived by switching on in JETSET a simple simulation of this effect (without changing other parameters). In this analysis both neutral objects and charged tracks have been used to compute the event shapes. The stability of the corrections for detector effects has been checked by repeating the analysis with charged tracks only and by recomputing the corrections. The shift in α_s has been taken as a measure of the uncertainty. Finally the fit range has been extended (reduced) at both sides by three bins, and the largest deviation from the default range taken as error. All systematic errors are summarized in Table 2.

3.5 Event Orientation

The integration over event shape variables is from a theoretical point of view more delicate, because in NLO framework used here, infrared divergiencies are present in the two-jet region. Therefore some cuts has to be applied in order to use the numerical prediction. This can also be seen as an advantage, since the impact on the event orientation is strongest for hard $q\overline{q}g$-events. As illustrated in Fig. 4, the distribution becomes significantly flatter for events with low thrust. This can be seen clearly in Fig.5, where the ratio of the lowest order expectation (which is independent of α_s) and the NLO prediction is shown together with the data.
Another method relies on an analytic calculation in NNLO QCD. In contrast to the numerical calculations with `EVENT2`, this next-to-next-to leading order prediction contains the lowest order process $Z \to q\overline{q}$, and also higher order corrections up to terms in α_s^2. In general the event orientation can be written as follows :

$$\frac{1}{\sigma}\frac{d\sigma}{d\cos\theta} = \frac{3}{4}\left(1+\cos^2\theta\right)\frac{\sigma_U}{\sigma} + \frac{3}{2}\left(1-\cos^2\theta\right)\frac{\sigma_L}{\sigma} \tag{2}$$

where σ_U is the transverse unpolarized, σ_L the longitudinally polarized cross section and σ is the sum of both. Both σ_U and σ_L depend on α_s in the following way [12]:

$$\sigma_L \;=\; 2(8\ln\frac{3}{2}-3)\; R\;\sigma_0\;\frac{\alpha_s}{\pi}\;C_F\;(1+l\frac{\alpha_s}{\pi}) \tag{3}$$

where $\sigma_0 = 4\alpha^2\pi/3s$ and R contains the vector couplings and axial-vector couplings of the Z-boson to the fermions and the propagator. The unpolarized cross section σ_U is obtained by subtraction of σ_L from the total cross section [13]:

$$\begin{aligned} \sigma_U &= \sigma - \sigma_L \\ \sigma &= \sigma_0 N_c \left(R_a \left[1 + d_1\frac{\alpha_s}{\pi} + d_2\left(\frac{\alpha_s}{\pi}\right)^2 \right] + R_v \left[1 + c_1\frac{\alpha_s}{\pi} + c_2\left(\frac{\alpha_s}{\pi}\right)^2 \right] \right) \end{aligned} \tag{4}$$

Here, R_v contains only the vector couplings and R_a the axial couplings. Note that both σ_U and σ_L depend on electroweak parameters via the couplings and the coefficients c and d. The formula (2) has been fitted to the data and α_s or equivalently σ_L are determined, although with large errors, since the QCD effects on the event orientation are small. The result is :

$$\alpha_s(M_Z^2) = 0.121 \pm 0.022_{\rm stat} \pm 0.011_{\rm syst}$$

$$\sigma_L/\sigma = (1.22 \pm 0.21_{\rm stat} \pm 0.11_{\rm syst})\; 10^{-2}$$

In Fig. 6 the result of the fit compared to the lowest order form and the corresponding systematic uncertainties are listed in Table 4.

4 Conclusion

The distribution of oriented event shapes has been measured and compared to next-to-leading order QCD predictions. Good agreement over the whole range of $\cos\theta$ is observed. Measurements of α_s using oriented event shapes are in good agreement with those obtained by a standard method with integrated event shapes. The preliminary result using the variable Y_3 is:

$$\alpha_s(M_Z^2) = 0.1161 \pm 0.0003_{\rm stat} \pm 0.0051_{\rm syst} \quad \text{(oriented event shapes)}$$

$$\alpha_s(M_Z^2) = 0.1156 \pm 0.0003_{\rm stat} \pm 0.0055_{\rm syst} \quad \text{(integrated event shapes)}$$

The analysis of the event orientation has demonstrated the expected flattening with respect to the lowest order $1 + \cos^2\theta$ form. This effect is of the order of 1 % in total and increases up to 10 % for events with $T_R < 0.8$. From a fit of the next-to-next-to leading order prediction to the inclusive event orientation, α_s and the relative contribution of the longitudinally polarized cross section to the total cross section are determined with large uncertainties.

Acknowledgments

We would like to acknowledge the helpful support of B. Lampe and M. Seymour in this work. We wish to thank our colleagues from the CERN accelerator divisions for the successful operation of LEP. We are indebted to the engineers and technicians in all our institutions for their contribution to the good performance of ALEPH. Those of us from non-member states thank CERN for its hospitality.

References

[1] B. Adeva et al., L3 Collaboration, Phys. Lett. **B263** (1991) 551.

[2] P. Abreu et al., DELPHI Collaboration, Phys. Lett. **B274** (1992) 498.

[3] W. Braunschweig et al., TASSO Collaboration, Zeit. Phys. **C47** (1990) 181.

[4] D. Decamp et al., ALEPH Collaboration, Nucl. Instr. and Meth. **A294** (1990) 121. '

[5] D. Buskulic et al., ALEPH Collaboration, Nucl. Instr. and Meth. **A360** (1995) 481.

[6] S. Catani et al., Phys. Lett. **B269** (1991) 432; W. J. Stirling, Durham Workshop, J. Phys. **G17** (1991) 1657.

[7] program EVENT2, M. Seymour.

[8] S. Catani and M. Seymour, CERN-TH-96/28.

[9] T. Sjöstrand, Comp. Phys. Comm. **39** (1986) 347; **43** (1987) 367; **82** (1994) 74.

[10] G. Marchesini et al., Nucl. Phys. **B310** (1988) 571; Comp. Phys. Comm. **67** (1992) 269.

[11] L. Lönnblad, Comp. Phys. Comm. **71** (1992) 465.

[12] B. Lampe, Phys. Lett. **B301** (1993) 435.

[13] J. H. Kühn and P. M. Zerwas., in "Z Physics at LEP 1", edited by G. Altarelli, CERN Yellow Report 89-08 (1989) 267.

Variable	Result on α_s
Y_3	$0.1161 \pm 0.0003 \pm 0.0051$
T_R	$0.1309 \pm 0.0004 \pm 0.0152$
B_W	$0.1202 \pm 0.0003 \pm 0.0065$
M_H	$0.1238 \pm 0.0004 \pm 0.0081$

Table 1: Results on α_s from oriented event shapes. The first error is the statistical one (including the error from limited Monte Carlo statistics), the second the total systematic error.

source of uncertainty	Y_3	T_R	B_W	M_H
Hadronization	± 0.0011	± 0.0057	± 0.0009	± 0.0028
Scale	± 0.0044	± 0.0137	± 0.0058	± 0.0067
Bose-Einstein	± 0.0012	± 0.0019	± 0.0011	± 0.0019
Detector resolution	± 0.0019	± 0.0019	± 0.0019	± 0.0019
Fit range	± 0.0003	± 0.0021	± 0.0017	± 0.0024
Total	± 0.0051	± 0.0151	± 0.0065	± 0.0081

Table 2: Systematic uncertainties on α_s from oriented event shapes.

Variable	Result on α_s
Y_3	$0.1156 \pm 0.0003 \pm 0.0055$
T_R	$0.1305 \pm 0.0005 \pm 0.0147$
B_W	$0.1199 \pm 0.0003 \pm 0.0070$
M_H	$0.1235 \pm 0.0004 \pm 0.0087$

Table 3: Results on α_s from integrated event shapes with the same systematic studies as for oriented event shapes.

source of uncertainty	$\Delta(\alpha_s)$
Hadronization	± 0.010
EW	± 0.002
Bose-Einstein	± 0.002
Detector resolution	± 0.001
Fit range	± 0.003
Total	± 0.011

Table 4: Systematic uncertainties for α_s from the event orientation, using the NNLO prediction.

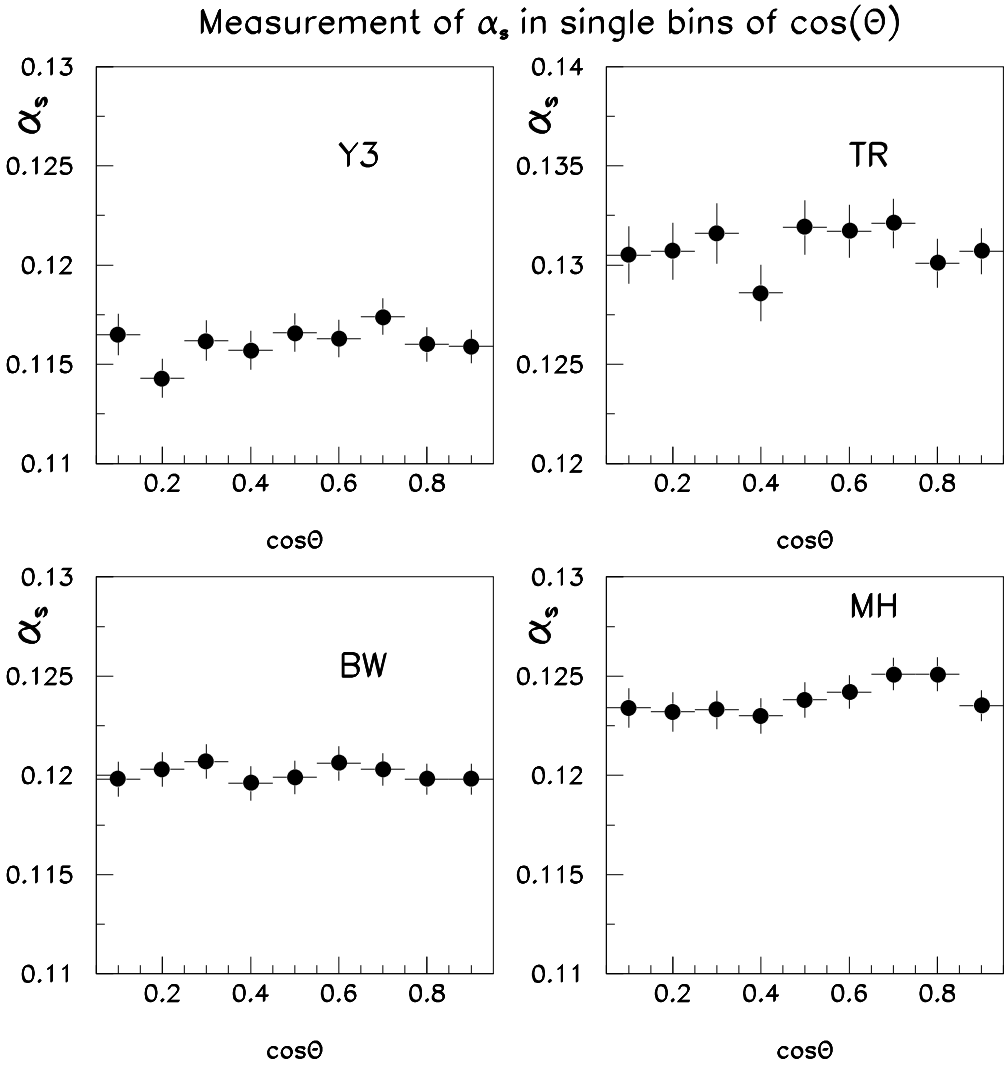

Figure 1: Measurement of α_s in single bins of $\cos\theta$ for four event shape variables. The fixed-order prediction with $\mu = M_Z/2$, corrected for hadronization with JETSET PS has been used.

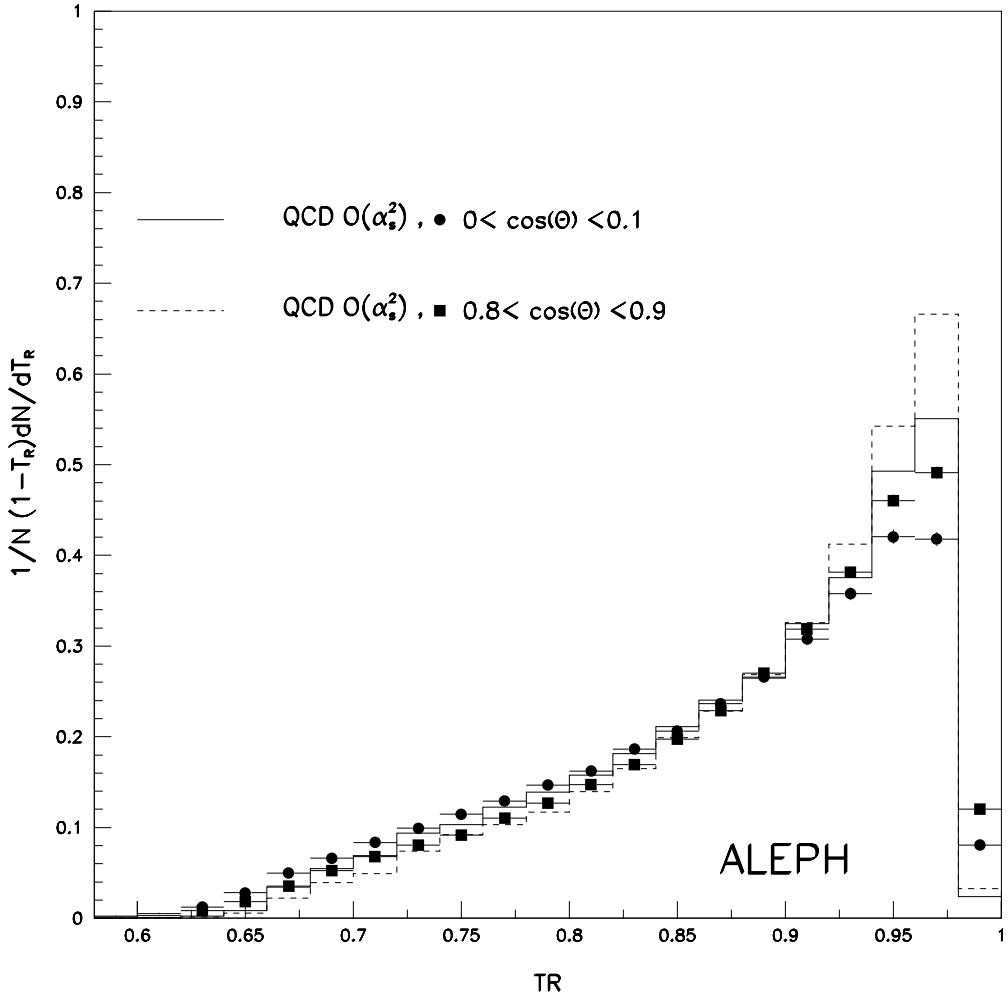

Figure 2: A fit of the theoretical prediction to the double differential cross section $1/N\ (1-T_R)d^2N/dT_R d\cos\theta$. The result of the fit is $\alpha_s = 0.1309 \pm 0.0004$. The parton shower model PS has been used for hadronization corrections. Note that the two curves shown are normalized to the number of events in that particular bin of $\cos\theta$, i.e. the trivial $1+\cos^2\theta$ form has been folded out.

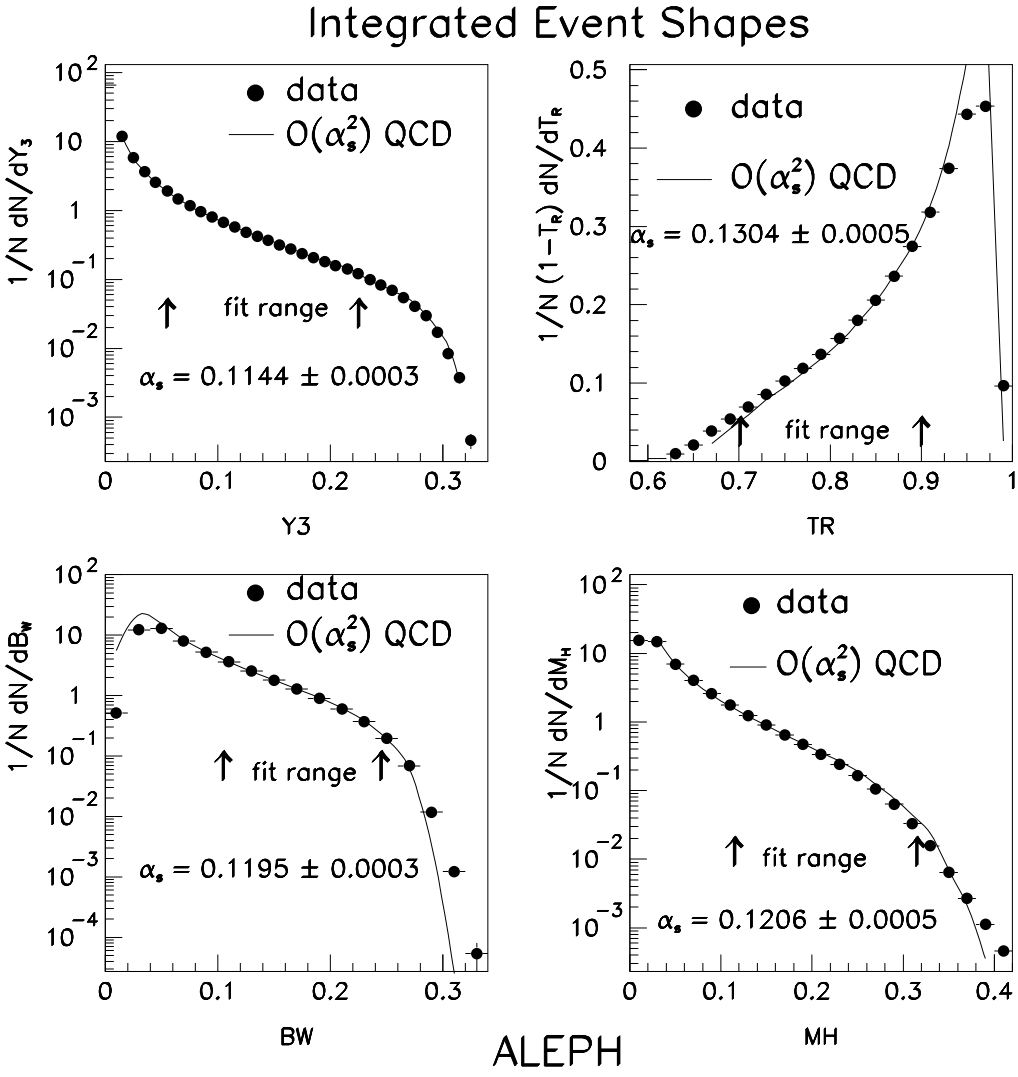

Figure 3: Integrated event shapes, compared to the NLO QCD prediction.

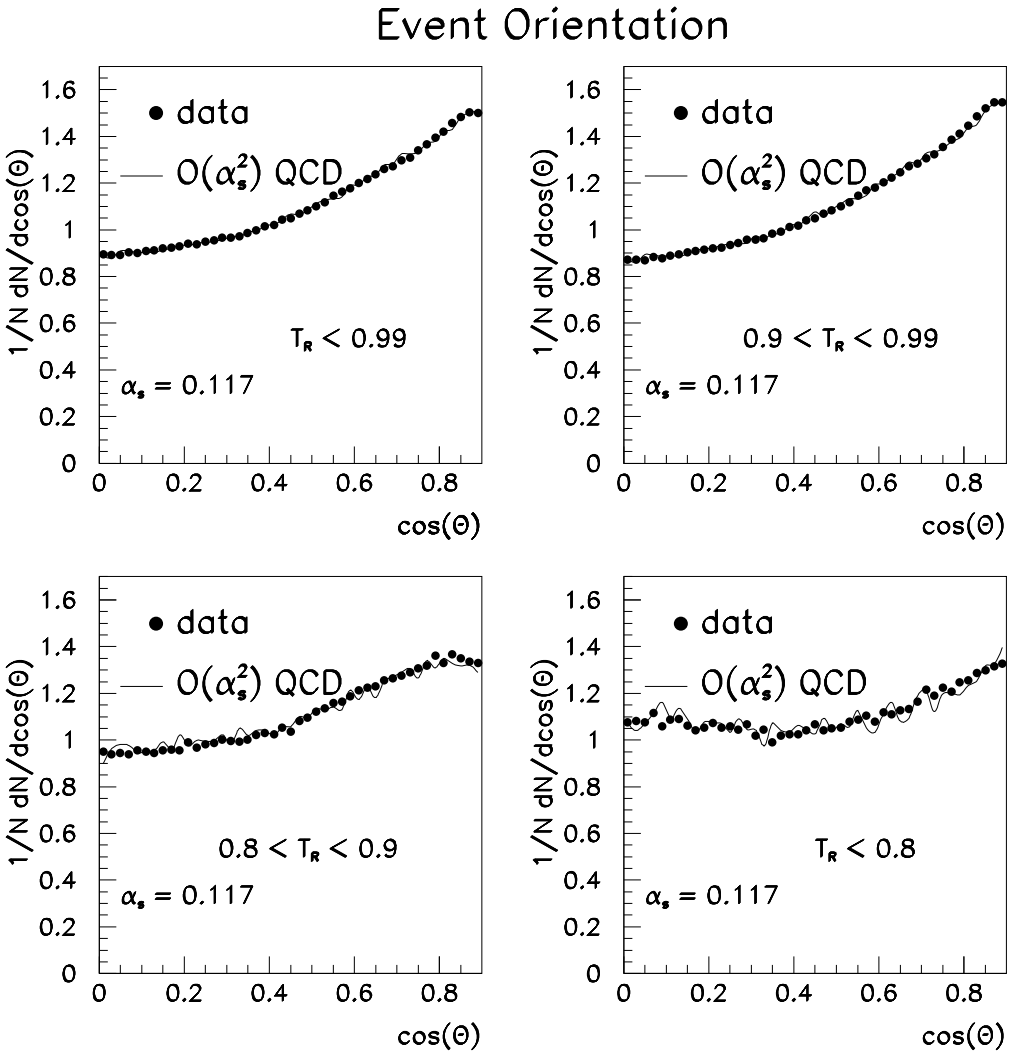

Figure 4: The event orientation for different cuts on T_R. In principal the prediction can be used to fit α_s, but since the number of events in a given range of T_R (used for normalization) depend also on α_s, a scan over α_s has to be done.

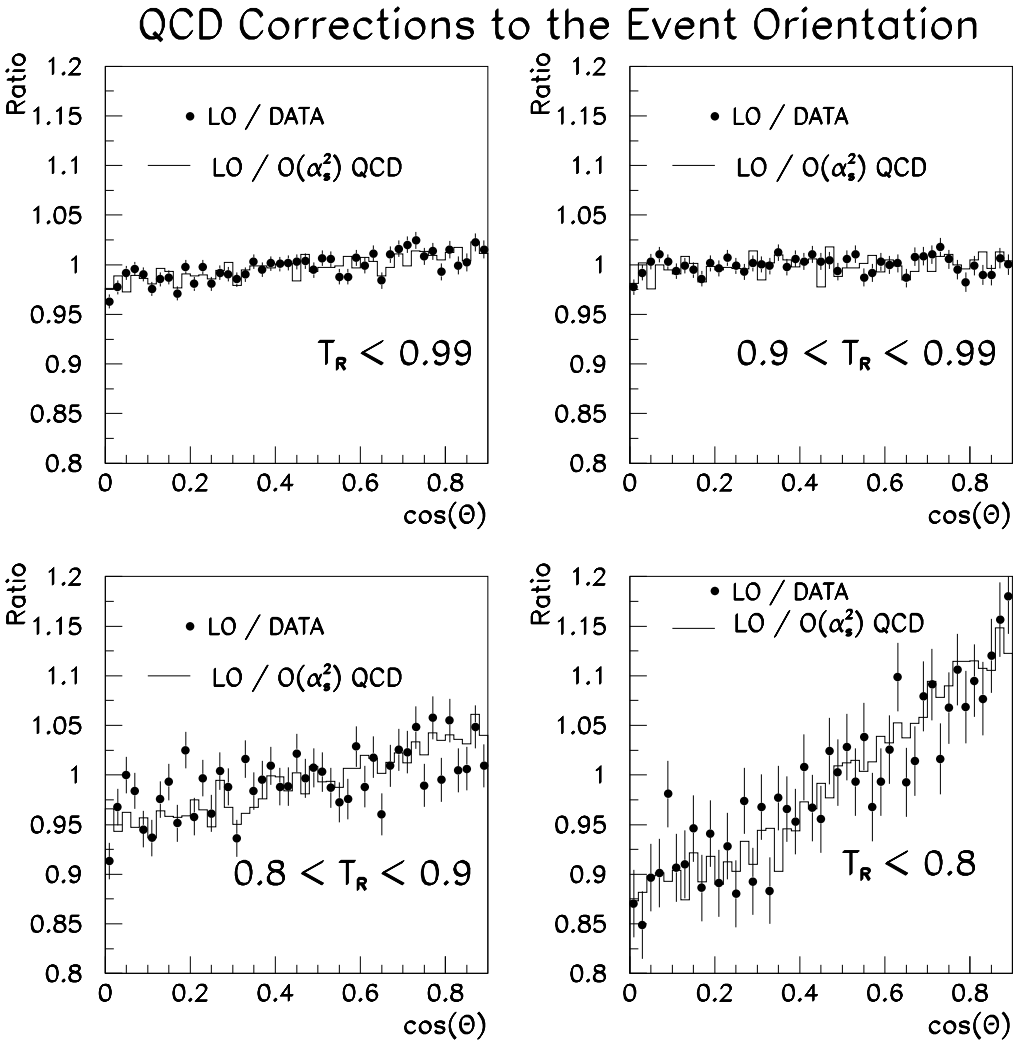

Figure 5: The ratio of the lowest order prediction ($\propto 1 + \cos^2\theta$, independent of α_s) and the next-to-leading order fit results shows the size of changes induced by higher order QCD processes.

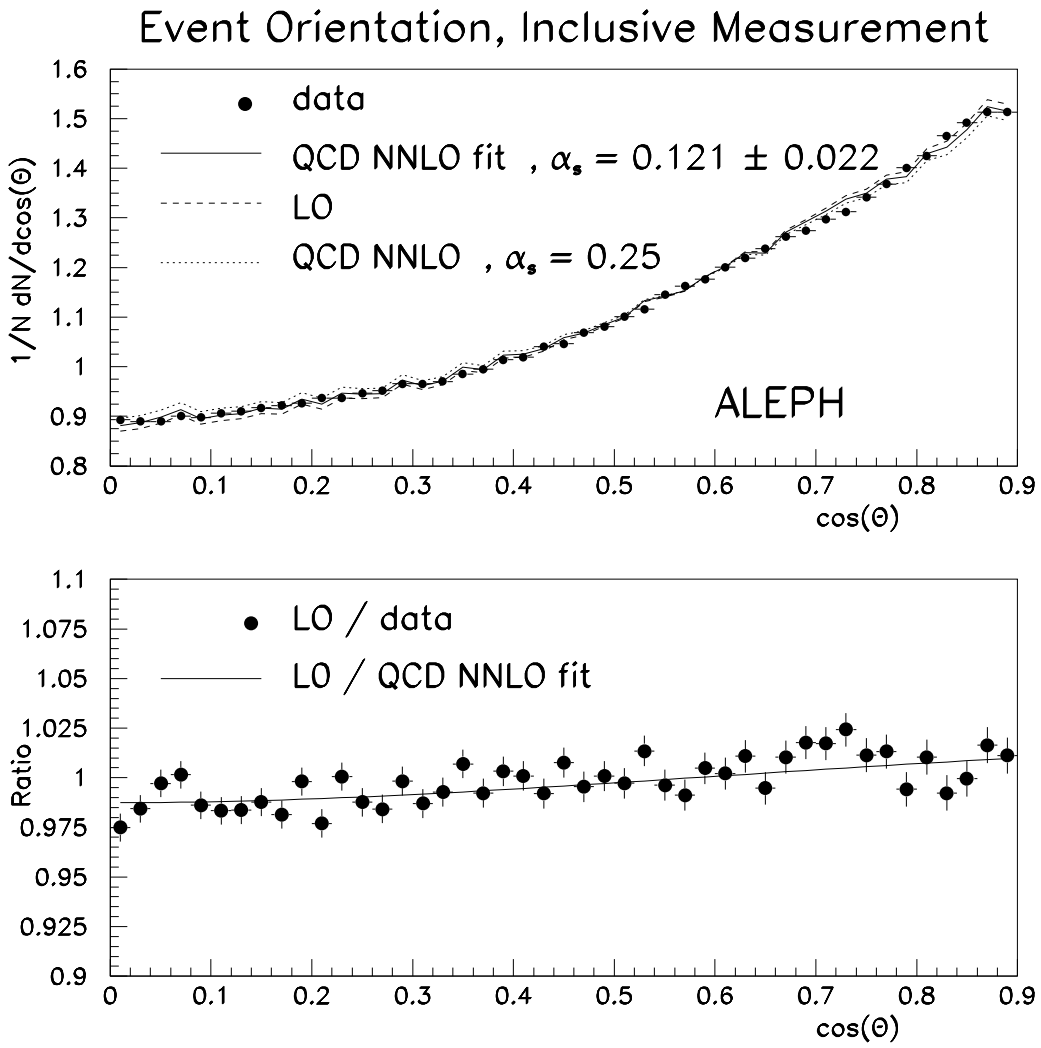

Figure 6: The inclusive distribution of $\cos\theta$ (without any cuts on T_R) is compared to next-to-next-to leading order calculation, which includes the lowest order process $Z \to q\overline{q}$ and higher order corrections up to terms in α_s^2. Note that the total χ^2 for the QCD fit is $\chi^2/d.o.f = 49/44$, which has to be compared with $\chi^2/d.o.f = 85/45$ for the lowest order expectation. A similar χ^2 is obtained when $\alpha_s = 0.25$ is used in the QCD formula. The lower plot shows the ratio of the $1 + \cos^2\theta$ form and both the QCD fit and the data. It can be seen that the flattening induced by QCD leads to a change in the distribution of the order of one %.